ADVANCED MATERIALS
www.advmat.de

Organic Long-Persistent Luminescence from a Thermally Activated Delayed Fluorescence Compound

Wenbo Li, Zhaoning Li, Changfeng Si, Michael Y. Wong, Kazuya Jinnai, Abhishek Kumar Gupta, Ryota Kabe, Chihaya Adachi, Wei Huang, Eli Zysman-Colman, and Ifor D. W. Samuel**

Organic long-persistent luminescence (OLPL) is one of the most promising methods for long-lived-emission applications. However, present room-temperature OLPL emitters are mainly based on a bimolecular exciplex system which usually needs an expensive small molecule such as 2,8-bis(diphenylphosphoryl)dibenzo[b,d]thiophene (PPT) as the acceptor. In this study, a new thermally activated delayed fluorescence (TADF) compound, 3-(4-(9H-carbazol-9-yl)phenyl)acenaphtho[1,2-b]pyrazine-8,9-dicarbonitrile (CzPhAP), is designed, which also shows OLPL in many well-known hosts such as PPT, 2,2′,2″-(1,3,5-benzinetriyl)-tris(1-phenyl-1-H-benzimidazole) (TPBi), and poly(methyl methacrylate) (PMMA), without any exciplex formation, and its OLPL duration reaches more than 1 h at room temperature. Combining the low cost of PMMA manufacture and flexible designs of TADF molecules, pure organic, large-scale, color tunable, and low-cost room-temperature OLPL applications become possible. Moreover, it is found that the onset of the 77 K afterglow spectra from a TADF-emitter-doped film is not necessarily reliable for determining the lowest triplet state energy level. This is because in some TADF-emitter-doped films, optical excitation can generate charges (electron and holes) that can later recombine to form singlet excitons during the phosphorescence spectrum measurement. The spectrum taken in the phosphorescence time window at low temperature may consequently consist of both singlet and triplet emission.

Long-afterglow emitters are a class of material that show long-lived emission lasting for seconds to even hours after the excitation source is removed.[1] Currently, high-performance long-lived materials are mainly based on inorganic materials such as $CaAl_2O_4$ or $SrAl_2O_4$ with rare metal dopants such as Eu, Nd, and Dy.[2,3] Although the emission can last for more than 10 h, the fabrication requires high temperature (>1000 °C) and the use of rare metals. Recently, purely organic long-afterglow materials have been discovered and they possess many advantages over their inorganic counterparts, including the use of more sustainable elements and lower fabrication costs. There are two main sub-classes of materials that show purely organic long-lived emission at room temperature: 1) room-temperature phosphorescence (RTP) materials and 2) organic long-persistent luminescence (OLPL) materials. RTP has been heavily studied in recent years.[4–7] Materials showing RTP typically have a large singlet–triplet-excited-state energy gap (ΔE_{ST}) to inhibit reverse

W. Li, Dr. A. K. Gupta, Prof. I. D. W. Samuel
Organic Semiconductor Centre
SUPA
School of Physics and Astronomy
University of St Andrews
North Haugh, St Andrews, Fife KY16 9SS, UK
E-mail: idws@st-andrews.ac.uk

Z. Li, C. Si, Dr. M. Y. Wong, Dr. A. K. Gupta, Prof. E. Zysman-Colman
Organic Semiconductor Centre
EaStCHEM
School of Chemistry
University of St Andrews
St Andrews, Fife KY16 9ST, UK
E-mail: eli.zysman-colman@st-andrews.ac.uk

The ORCID identification number(s) for the author(s) of this article can be found under https://doi.org/10.1002/adma.202003911.

DOI: 10.1002/adma.202003911

Z. Li, Prof. W. Huang
Key Laboratory of Flexible Electronics (KLOFE) and Institute of Advanced Materials (IAM)
Nanjing Tech University (NanjingTech)
30 South Puzhu Road, Nanjing 211800, China

K. Jinnai, Prof. R. Kabe, Prof. C. Adachi
Center for Organic Photonics and Electronics Research (OPERA)
Kyushu University
744 Motooka, Nishi-ku, Fukuoka 819-0395, Japan

K. Jinnai, Prof. R. Kabe, Prof. C. Adachi
JST
ERATO
Adachi Molecular Exciton Engineering Project
Kyushu University
744 Motooka, Nishi-ku, Fukuoka 819-0395, Japan

Prof. R. Kabe
Organic Optoelectronics Unit
Okinawa Institute of Science and Technology Graduate University
1919-1 Tancha, Onna-son, Okinawa 904-0495, Japan

Prof. C. Adachi
International Institute for Carbon Neutral Energy Research (WPI-I2CNER)
Kyushu University
744 Motooka, Nishi-ku, Fukuoka 819-0395, Japan

intersystem crossing (RISC), and also are in a rigid environment such as a crystalline lattice where non-radiative decay processes are strongly inhibited.[8–10] The longest reported RTP emitters have photoluminescence (PL) lifetimes, of over 23 s.[11] Compared with RTP, there are only a small handful of examples of OLPL materials.[12–14] The afterglow duration for materials showing OLPL is significantly longer, lasting thousands of seconds. Further, the material is not required to be in a crystalline state to show OLPL.[12]

Solid-state room-temperature OLPL was first reported by Ohkita et al. between 1997 and 2001. They found that doping perylene into poly(*n*-butyl methacrylate) (PnBMA) resulted in films showing afterglow lasting around 200 s.[15,16] Long-afterglow room-temperature OLPL was first reported by Kabe et al. in 2017.[14] They demonstrated that doping 1 mol% *N*,*N*,*N*′,*N*′-tetramethylbenzidine (TMB) into 2,8-bis(diphenyl-phosphoryl) dibenzo[b,d]thiophene (PPT) can produce an exciplex emitter showing an afterglow of more than 1 h. In 2018, the same group demonstrated that a 4,4′,4″-tris[phenyl(*m*-tolyl)amino]-triphenylamine (m-MTDATA):PPT exciplex showed a twofold longer afterglow under the same conditions compared with TMB:PPT.[12] Moreover, they realized multi-color OLPL by doping different fluorescent chromophores into the TMB:PPT system.[17] Expanding this concept further, the same group fabricated low-cost OLPL materials using the exciplex formed by TMB and PBPO, an n-type polymer. The corresponding plastic film showed an afterglow lasting around 7 min.[13] In terms of the OLPL formation condition, Lin et al. asserted that a small energy gap between the singlet charge transfer state (^{1}CT) and the triplet locally excited state (^{3}LE) in an exciplex system is desirable as this helps to create more photoinduced charges through the ^{1}CT exciton dissociation.[18]

Here, we demonstrate that exciplex formation is not required for room-temperature OLPL as it can be obtained through doping of a thermally activated delayed fluorescence (TADF) compound into common host materials such as poly(methyl methacrylate) (PMMA) and 2,2′,2″-(1,3,5-Benzinetriyl)-tris(1-phenyl-1-H-benzimidazole) (TPBi), as well as PPT. We studied the TADF properties of a molecule, 3-(4-(9H-carbazol-9-yl) phenyl)acenaphtho[1,2-b]pyrazine-8,9-dicarbonitrile (CzPhAP), and its application for OLPL. 0.5 wt% CzPhAP-doped films in PPT and TPBi show OLPL with an afterglow duration of more than 1000 s, and the afterglow duration is over 400 s when it is doped in PMMA. This discovery is important because it enables a wide range of host materials to be used for OLPL including inexpensive and easily molded polymers such as PMMA. A further feature of our study is that the relatively large ΔE_{ST} found in this TADF emitter enables us to study the evolution of the emission spectra over time and so clearly identify the excited state responsible for the emission in each time window. Within that, the low-temperature PL spectrum study of this OLPL system reveals that the onset value of the 77 K afterglow spectrum from a TADF-emitter-doped film cannot necessarily be reliable for determining the energy level of the lowest triplet excited state (T_1) of the TADF emitter. This is because even in the phosphorescence time window at 77 K, singlets may still be generated continuously by charge recombination in the film and the consequent 77 K afterglow spectrum may consist of both the lowest singlet state (S_1) and T_1 emission.

We designed CzPhAP as a TADF emitter. This compound consists of a carbazole (Cz) donor group linked by a paraphenylene bridge to a strongly electron-accepting acenaphtho[1,2-b]pyrazine-8,9-dicarbonitrile (AP). AP has previously been employed in red TADF emitter design and based on its rigid character, OLEDs using AP-based emitters show high efficiency.[19–22] The related molecular structures and performance of these AP-based emitters are summarized in Table S1, Supporting Information. Here, the DFT and TDDFT calculations show that CzPhAP possesses a large calculated ΔE_{ST} of 0.18 eV (**Figure 1**a). The HOMO and LUMO energies for CzPhAP, determined experimentally from cyclic voltammetry (CV) and differential pulse voltammetry (DPV) measurements in acetonitrile (Figure S15, Supporting Information), are −5.75 and −3.65 eV, respectively. For comparison, ambient pressure photoemission spectroscopy (APS) of a neat film of CzPhAP gave a HOMO level of −5.76 eV (Figure S16, Supporting Information), which aligns with the DPV-determined level.

The steady-state absorption spectrum of CzPhAP in toluene features a broad, low-energy absorption band at 425 nm that is assigned to a CT transition (Figure 1b). The steady-state PL spectra also feature a CT state characteristic: emission is generally broad and featureless and positive solvatochromism is observed. The ΔE_{ST}, determined from the difference in energy between the onsets of the prompt fluorescence and phosphorescence spectra obtained in toluene glass at 77 K (Figure 1c), is 0.47 eV, which is much larger than that predicted by the DFT. Because of this large ΔE_{ST}, CzPhAP does not show TADF properties in toluene and the time-resolved PL (TRPL) decay curve in toluene shows no delayed component (Figure S17, Supporting Information). However, singlet emission quenching by O_2 is still observed in these TRPL decay curves, which is also reflected in the PL quantum yield (Φ_{PL}) measurement in toluene (Φ_{PL} is 84% under degassed condition and 75% when aerated). The solution-state photophysical data is summarized in Table S2, Supporting Information.

We next investigated the photophysical properties of the doped thin films of CzPhAP in two OLED-relevant hosts, PPT and TPBi, as well as PMMA (**Figure 2**a). The HOMO and LUMO energy levels of all of these materials are presented in Figure 2a to exclude the possibility of exciplex formation between the hosts and the guest. The doping concentrations are 6 wt% for the PPT film and 10 wt% for the TPBi and PMMA films. The steady-state emission spectra of the PPT, TPBi, and PMMA films have broad CT features with emission maxima of 586, 578, and 560 nm (Figure 2b). The absolute Φ_{PL}'s of these films are 56.6%, 47.4%, and 32.4%, respectively, under a nitrogen atmosphere. The Φ_{PL} values dropped slightly to 49.9%, 46.2%, and 29.1% in air. The reduction of the Φ_{PL} in air is attributed to quenching by oxygen. The reduction is smaller than in many TADF materials because of the low reverse intersystem cross rate (k_{RISC}) caused by the large ΔE_{ST}, 0.24 eV, as measured in the 6 wt% CzPhAP:PPT film (Figure 2c). Figure 2c shows the prompt and afterglow emission spectra of the 6 wt% CzPhAP:PPT film measured at 77 K. The afterglow spectrum (red line) for T_1 determination has a shoulder (at 577 nm) with the same peak position as the prompt emission spectrum (black line), and this shoulder is assigned to singlet emission through charge recombination, which is discussed in detail below.

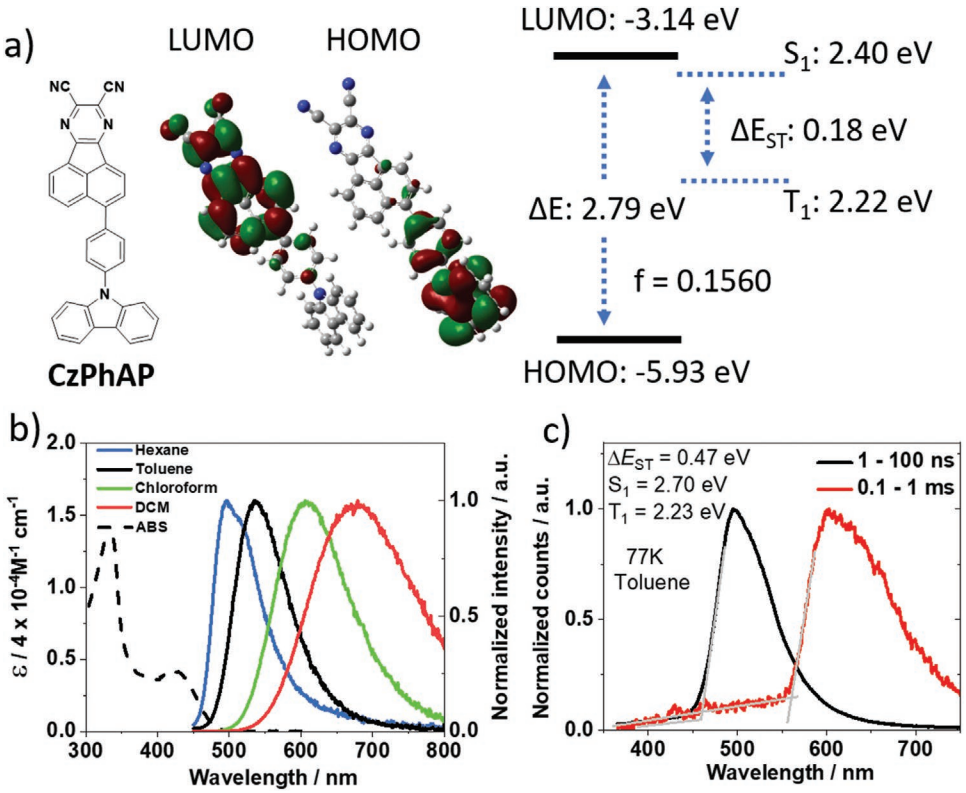

Figure 1. The calculation results of CzPhAP and its emission and absorption spectra in solution. a) Molecular structure, DFT-determined electron density distribution, and energies of the HOMO and LUMO, and TDDFT-determined energies of the S_1 and T_1 states of CzPhAP in the gas phase. b) Steady-state absorption spectrum in toluene and photoluminescence solvatochromism study of CzPhAP (λ_{exc} = 340 nm). c) 77 K PL prompt and phosphorescence spectra of CzPhAP in toluene (λ_{exc} = 343 nm); the ΔE_{ST} value is taken from the onset value difference between the two spectra.

Therefore, the onset value of the PPT film's phosphorescence spectrum was taken from extrapolating the curve from the main peak (at 629 nm) rather than the shoulder. All the solid-state photophysics data are compiled in Table S3, Supporting Information. Figure S18, Supporting Information, shows the temperature-dependent TRPL decay curves (from 300 to 100 K) of this PPT film. The delayed emission was gradually quenched with the decreasing temperature, demonstrating that the TADF is still operating in CzPhAP when it is doped in PPT (even though the ΔE_{ST} = 0.24 eV).

OLEDs employing 6 wt% CzPhAP:PPT as the emission layer (EML) were fabricated and the device structure and performance are shown in Figure 2d and Figure S19, Supporting Information. The OLED shows a broad electroluminescence (EL) emission spectrum with λ_{EL} at 570 nm, CIE coordinates of (0.47, 0.51), and EQE_{max} of 11%. This high EQE_{max} value confirms that TADF is contributing to the emission of CzPhAP in the polar solid host PPT. There is significant efficiency roll-off with an EQE of 2.8% at 100 cd m^{-2}, which is the result of the large ΔE_{ST} and the correspondingly small k_{RISC}. There may also be singlet-polaron and triplet-polaron quenching that is contributing to the efficiency roll-off. Its relevance to the phenomenon of charge accumulation in the EML is discussed below.

During our solid-state photophysical investigation, we observed that the TRPL decay durations of the CzPhAP-doped films are dependent on the excitation durations (measured by Edinburgh Instrument FLS 980). Figure 2e shows the TRPL decay measurement result of the 6 wt% CzPhAP:PPT film measured under vacuum at room temperature using different numbers of excitation shots. The excitation source was a 378 nm pulsed picosecond laser driven in burst mode (the time interval between two shots is 10 ns and the pulse duration of each shot is around 200 ps FWHM). When the number of the excitation shots was increased, the excitation duration was also correspondingly increased, and the consequent delayed emission durations were also extended as observed in the normalized TRPL decay curves (Figure 2e). Furthermore, the slopes of the decay curves vary with different numbers of excitation shots, indicating the emission process is more complicated than typical TADF or RTP. Recently, Yamanaka et al.[24] reported that in the TRPL decay measurements of a TPA-DCPP:CBP film, they could extend the PL decay duration of the film from around 0.5 ms to more than 2 ms by increasing the excitation duration from 10 to 500 µs. They proved that the origin of this phenomenon is the photoinduced charge generation during the excitation process. When the excitation source is off, these charges recombine and contribute to the delayed emission. Therefore, the photoinduced charges are likely to be the reason for the extended delayed emission here. However, Yamanaka et al. only focused on demonstrating the existence of photoinduced charges in their films but did not observe long delayed emission lasting over a second, and so they did not report the OLPL from their films. In contrast, as shown in Figure 2f, with 10 000 excitation shots (equals 2 µs excitation duration), all of the

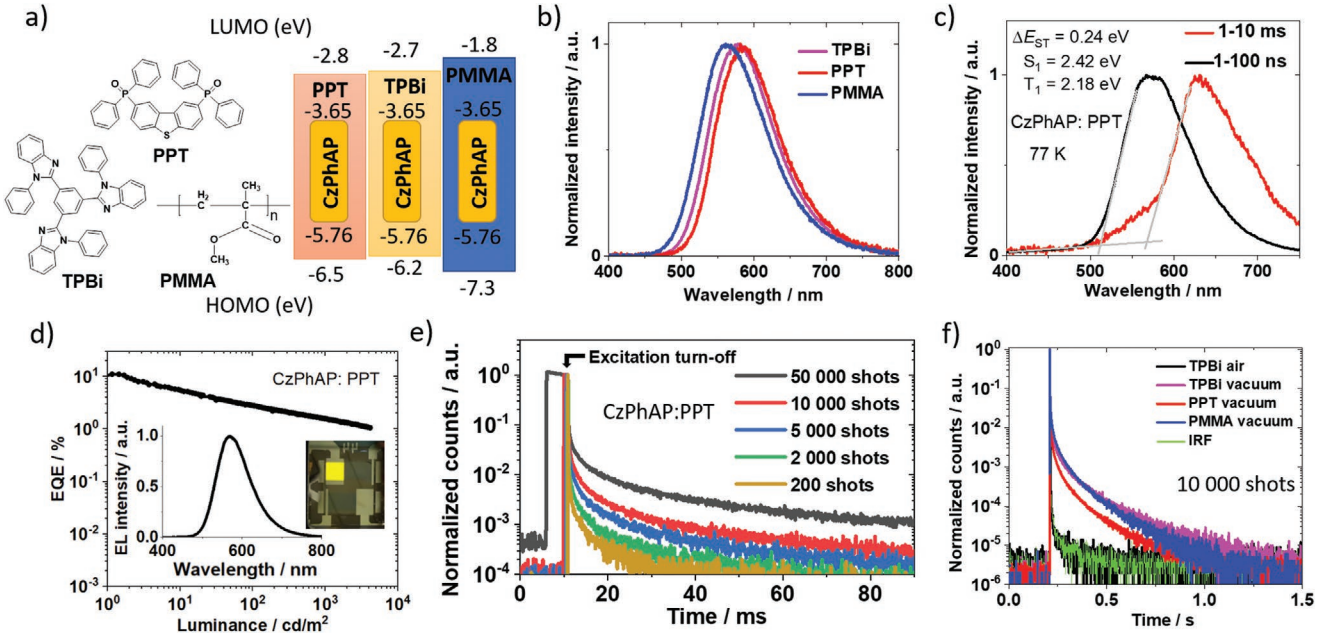

Figure 2. The PL and EL properties of CzPhAP in solid state. a) Molecular structures and HOMO/LUMO energy diagrams of CzPhAP, PPT, TPBi, and PMMA. The HOMO and LUMO values of PPT, TPBi, and PMMA are taken from refs. [14], [4], and [23], respectively. b) Steady-state PL emission of the 10 wt% CzPhAP:TPBi/PMMA films and the 6 wt% CzPhAP:PPT film. c) 1–100 ns prompt fluorescence and 1–10 ms afterglow spectra of the 6 wt% CzPhAP:PPT film at 77 K. The ΔE_{ST} value is determined from the difference in the onset values of the fluorescence and phosphorescence spectra. d) Device *EQE* versus luminance (inset: normalized EL spectrum, device in operation and a photograph of the OLED). e) TRPL decay curves of the 6 wt% CzPhAP:PPT film with different numbers of excitation shots. (Excitation source: 378 nm picosecond laser). f) TRPL decay of the 6 wt% CzPhAP:PPT and 10 wt% CzPhAP:TPBi/PMMA films measured in air and under vacuum with 10 000 excitation shots. (Excitation source: 378 nm picosecond laser).

CzPhAP:PPT/TPBi/PMMA films showed emission lasting up to 1 s, which is much longer than that reported by Yamanaka et al. Furthermore, this delayed emission is oxygen sensitive and is entirely quenched when the film is exposed to air as can be observed from the decay curve of the TPBi film.

To further investigate the properties of the weak and long-lived delayed emission from CzPhAP, we fabricated much thicker amorphous films (≈1 mm) using PPT and TPBi as the hosts through melt-casting of mixed host–guest powder on glass substrates in the same manner as described by Kabe et al.[14] While, the thick PMMA film was obtained from polymerization from PMMA's monomer. Thicker films are better for the study of afterglow because they absorb more light and generate stronger emission for afterglow detection. In addition, we decreased the doping concentrations of these films because Kabe et al.[14] had previously shown that a lower doping concentration is better for obtaining longer OLPL durations. However, in blends where FRET occurs from host to emitter, too low a concentration will lead to insufficient FRET. Therefore, 0.5 wt% was chosen as the emitter doping concentration of these thick films. Furthermore, as shown in Figure 2e, longer excitation duration can also help to extend the afterglow duration. Therefore, these thick films were excited by a 365 nm LED for 60 s (for the PPT and TPBi films) or 1000 s (for the PMMA film) before the PL decay measurement. The long-lived afterglow was measured by a silicon photomultiplier (SiPM) connected to a multimeter. **Figure 3**a shows the PL decay traces of the 0.5 wt% CzPhAP:PPT/TPBi/PMMA films measured under vacuum at room temperature 1 s after the excitation, so as to avoid the strong prompt emission. Both the PPT and TPBi films show average emission duration over 1000 s, while the PMMA film shows emission duration over 400 s. The long-lived afterglow from PPT and TPBi films demonstrate that doping a TADF compound into common hosts can have comparable emission duration to that of state-of-the-art OLPL systems at room temperature.[14] The decay curves of the PPT and TPBi films start to follow power law from 5 s after photoexcitation, and the PMMA film follows a power law from 7 s after excitation. Power law decay is a feature of OLPL that originates from photoinduced charges. This suggests the mechanism of the long-lived afterglow in our systems is also OLPL, which is similar with that of the previously reported OLPL materials.[13,14] Importantly, we observe this phenomenon originating from a donor–acceptor type TADF compound, while in the previous reports,[12–14] this process occurred in materials that form exciplexes.

As shown in Figure 3a, linear fits of the power law decay components in log–log scale yield slope values of –0.98 for films of CzPhAP:PPT, –1.00 for CzPhAP:TPBi, and –0.55 for CzPhAP:PMMA, respectively, indicating photoinduced charges are recombining at different rates in these films. The origin of different slope values in long-persistent luminescence (LPL) has been studied in between early 1950s and late 1990s. At that time, LPL was often called isothermal luminescence. The models can be divided into those based on electron diffusion, and those based on electron tunneling. The diffusion model was first proposed by Debye and Edwards[25] in 1952. In this model, the positively charged emitter radicals are treated as electron sinks with many photoinduced electrons around the radicals after photoexcitation. The radicals are normally much larger and heavier than the electrons, so they are considered to be firmly held by the solid media and cannot move, whereas the

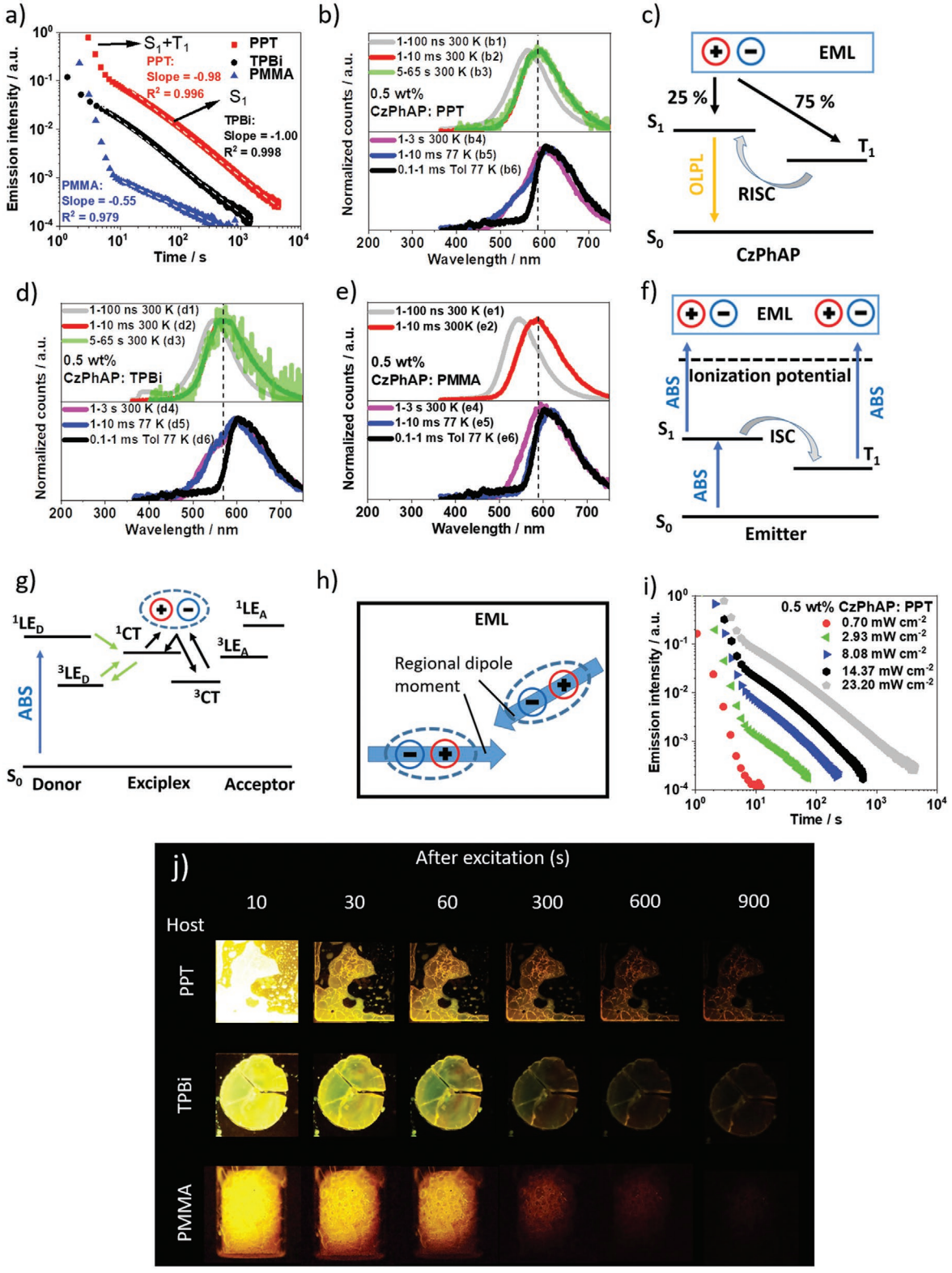

Figure 3. The OLPL properties of CzPhAP. a) OLPL decay curves of the 0.5 wt% CzPhAP:PPT/TPBi/PMMA films measured under vacuum at room temperature (λ_{exc} = 365 nm, excitation intensity and durations: 23.20 mW cm^{-2}, 60 s; 7.30 mW cm^{-2}, 60 s; 23.20 mW cm^{-2}, 1000 s). b,d,e) TRPL spectra of the 0.5 wt% CzPhAP:PPT/TPBi/PMMA films and CzPhAP in toluene (λ_{exc} = 343 nm). c) Schematic diagram of the charge recombination and OLPL emission process in the CzPhAP-doped films. f–h) Schematic diagrams of successive two-photon ionization, CT charge dissociation (figure adapted from ref. [18]), and spontaneous orientation polarization (SOP). i) Excitation intensity-dependent OLPL decay curves of the 0.5 wt% CzPhAP:PPT films measured under vacuum at room temperature (λ_{exc} = 365 nm, excitation duration: 60 s). j) Photographs of the OLPL of the 0.5 wt% CzPhAP:PPT/TPBi/PMMA films (λ_{exc} = 365 nm).

ejected electrons are assumed to be able to diffuse in one direction through the solid. This model was later improved by Abell and Mozumder[26] in 1972 through strict mathematical derivation, and the conclusion was that, within the electron diffusion model, a slope value of –1 can be obtained at the intermediate state of an OLPL decay, but the slope value will finally go to –1.5 at a longer time scale. Hamill and Funabashi[27] developed a diffusion model for LPL using the hopping time distribution of a continuous-time random walk (CTRW) used by Scher and Montroll[28] to explain the long tail of the transient photocurrent in amorphous solids. This model leads to slower electron diffusion and a lower rate of charge recombination, with a slope of the PL decay between 0 and –1. An alternative approach is the electron tunneling model, in which electrons recombine with the emitter radicals by tunneling, a process that is independent of temperature. In 1975, Tachiya and Mozumder[29] concluded that, within this model, the slope value should be close to –1. Therefore, the slope values predicted by these three charge-recombination models, namely electron diffusion, CTRW, and electron tunnelling, are [–1.5, –1], (0, –1), and close to –1, respectively. Our measured slopes for all 3 hosts are compatible with the model of Hamill and Funabashi. As all models can explain a slope of –1, our results in PPT and TPBi hosts could also be explained by the other models. However, the main focus of our work is to demonstrate room-temperature OLPL can be realized in TADF-emitter-doped films, and that it has similar afterglow duration to exciplex OLPL emitters.

It is noteworthy that all the TRPL decay curves in Figure 3a show two decay regimes. For the PPT and TPBi films, one regime is between 1–5 s, and the other is after 5 s; For the PMMA film, one regime is between 1–7 s and the other is after 7 s. To investigate the origin of these two regimes, TRPL spectra of these films were collected under vacuum in different time windows so as to identify the emitting species in each time window. Figure 3b shows the TRPL spectra of the 0.5 wt% CzPhAP:PPT film measured under vacuum in the time windows of 1–100 ns, 1–10 ms, 1–3 s, and 5–65 s after excitation at 300 K and in the time window of 1–10 ms after excitation at 77 K. We then compared these five PL spectra to CzPhAP's phosphorescence spectrum measured in flash cooled toluene glass at 77 K. In order to refer to the spectra in Figure 3b easily, we have labeled them b1–b6. The comparison of spectra presented in Figure 3b (top) reveals that the PL emission of the PPT film in the second regime (>5 s) originates from S_1: the broad and structureless PL spectrum collected in the time window of 1–100 ns (spectrum b1) is the prompt S_1 emission. The PL spectrum collected in the 1–10 ms window, b2, is from the TADF of the emitter, which is also from S_1. Spectrum b2 is modestly redshifted compared to spectrum b1, which is commonly observed in TADF materials. This redshift is caused by the conformational relaxation of the host and emitter.[30] Spectrum b3 shows a perfect overlap with spectrum b2, indicating that spectrum b3 also comes from S_1. Therefore, the emission of the OLPL from 5 s after excitation also originates from the S_1 of CzPhAP, which is labeled in Figure 3a. This is understandable because OLPL comes from charge recombination. As shown in Figure 3c, when the charges recombine, the generated triplets can be converted into singlets through TADF so that only singlet emission is observed in the power law decay regime.

The comparison of spectra in Figure 3b (bottom) reveals that the PL emission of the PPT film in the first decay regime (1–5 s) is from both the S_1 and T_1 states of CzPhAP. Figure 3b (bottom) shows the effect of temperature on spectra b4, b5, and b6. Spectra b4 and b5 have similar profiles, implying similar species are contributing to both of the spectra regardless of the huge temperature and time window differences. Also, spectrum b5 has a peak at 608 nm and a shoulder at 584 nm, indicating more than one species is emitting. To identify these species, spectra b5 and b6 were compared. As spectrum b6 is the phosphorescence spectrum of CzPhAP collected in 77 K toluene glass, it can be assigned to be purely from the T_1 of CzPhAP. In addition, it can be seen in Figure 3b (bottom) that (on the right side of the black dashed line) the lower energy component of spectra b5 and b6 show a perfect overlap. Therefore, the peak of spectrum b5 (at 608 nm) is also from T_1. The shoulder at 584 nm was found to come from the S_1 state: as shown in Figure S22c, Supporting Information, the higher-energy component of spectrum b5 (on the left side of the black dashed line) is composed of spectra b1 and b2 which are both from S_1. Therefore, spectrum b5 is a superposition of emission from both S_1 and T_1. Moreover, as the spectrum b5 is similar to b4, it can be concluded that spectrum b4 also contains S_1 and T_1 emission. As spectrum b4 was collected in the 1–3 s time window at 300 K, the emission in the first decay regime (1–5 s) should also come from the S_1 and T_1, which is labeled in Figure 3a. These observations are also in line with those of Lin et al.[18]

Importantly, as has been discussed in spectrum b5, singlet emission can still be observed in the 1–10 ms time window at 77 K in the 0.5 wt% CzPhAP:PPT film (similar to the result shown in Figure 2c). Singlet generation is unlikely to be from RISC because of the low temperature and CzPhAP's large ΔE_{ST}. Therefore, the population of S_1 is not a TADF process, and we instead assign it to photoinduced charge generation and subsequent charge recombination. The choice of this mechanism is based on the fact that OLPL has been proven to play an important in the PPT film. Also, people have shown many cases of charge recombination at low temperature (<77 K).[14,15,31,32] Within this mechanism, there is a 25% probability of singlet exciton generation when the charge recombination occurs. Therefore, charge recombination is most likely to be responsible for the singlet generation here. Consequently, according to the analysis of spectrum b5, the onset of the 1–10 ms 77 K afterglow spectrum from a TADF-emitter-doped film is not necessarily a reliable indicator of the TADF emitter's T_1 energy level because it may contain some singlet emission, which would lead to an underestimation of ΔE_{ST}.

Similar behavior of the TRPL spectrum was observed in the 0.5 wt% CzPhAP:TPBi film, which is shown in Figure 3d and Figure S23c, Supporting Information. However, the spectral evolution of the 0.5 wt% CzPhAP:PMMA film at 77 K is different. Figure 3e (bottom) compares its spectra collected in the 1–3 s time window at 300 K (e4), in the 1–10 ms time window at 77 K (e5), and the phosphorescence spectrum measured in toluene (e6). It can be seen that spectrum e5 almost completely matches spectrum e6, indicating that the same emitting species is contributing to these two spectra. As has been discussed, spectrum e6 is purely from T_1, therefore, T_1 emission

also dominates spectrum e5. Consequently, in contrast to the CzPhAP:PPT/TPBi films, the onset of the CzPhAP:PMMA film's spectrum collected in the 1–10 ms time window at 77 K is almost purely from T_1, and so can be used to determine the T_1 energy level of CzPhAP. This indicates the charge-recombination rate in the 77 K PMMA film is much lower than those in the PPT and TPBi films, and so the intensity of the S_1 emission in the 0.5 wt% CzPhAP:PMMA film is negligible compared with that of the phosphorescence in the 1–10 ms time window at 77 K.

At 300 K, the spectral evolution behavior of the 0.5 wt% CzPhAP:PMMA film is similar with those of the 0.5 wt% films of CzPhAP in PPT and TPBi. Figure 3e (top) compares the spectra at 300 K in the 1–100 ns (e1) and 1–10 ms (e2) time windows. However, the spectrum after 7 s was not obtained because its low emission intensity is out of the measurement range of our spectrometer which is less sensitive compared with the SiPM for the PL intensity measurement. Figure 3e (top) shows that, in the PMMA film, the spectral evolution between the prompt and delayed emission is similar to that observed in the PPT and TPBi films. Also, Figure 3e (bottom) and Figure S24c, Supporting Information, show that spectrum e4 is composed of spectra e1, e2, and e6, which is similar to the cases of PPT and TPBi as well. Therefore, the emission in the first decay regime (1–7 s) of the PMMA film is also composed of the S_1 and T_1 emission.

In summary, there are three main conclusions from the spectral evolution study: 1) In the 300 K PPT and TPBi films, the OLPL emission in the second decay regime (>5 s) mainly originates from the S_1 of CzPhAP. 2) In all of these three films at 300 K, the emission in the first decay regime (1–5 s for the PPT and TPBi films, and 1–7 s for the PMMA film) has contributions from both S_1 and T_1. 3) Singlets are continuously generated at 77 K in the CzPhAP:PPT/TPBi films through charge recombination in the 1–10 ms time window. Therefore, the onset values of the shoulders of these two spectra cannot be used to determine the T_1 energy level of CzPhAP.

Although OLPL can be found in CzPhAP-doped films due to the existence of photoinduced charges, the mechanism of the charge-separation process and how it is related to CzPhAP's TADF properties are not entirely clear. So far, three photoinduced charge-separation mechanisms have been proposed within OLPL: successive two-photon ionization, CT exciton dissociation, and spontaneous orientation polarization (SOP) (schematic diagrams: Figure 3f–h, respectively). The successive two-photon ionization model was usually used by Ohkita et al.[15,32,33,34] in between 1996–2001. In this model, as shown in Figure 3f, emitters are first populated to their excited states (S_1 or T_1) and then absorb a second photon, which leads to ionization. In Ohkita's experiment,[31] a 351 nm XeF femtosecond laser (30 mJ cm^{-2}, 20 nm FWHM) was used to excite a TMB:PMMA film, and OLPL was observed from the film lasting for more than 2 h at 20 K.

In 2017, Kabe et al.[14] started to use exciplex systems for OLPL and significantly improved the OLPL intensity and duration at room temperature. Their charge-separation model (Figure 3g) is based on CT exciton dissociation, which is reminiscent of solar cell models:[18] the excitons at CT states can spontaneously dissociate into electrons and holes. The advantage in this model is that the charge separation is a one-photon process, which only requires a weak excitation source when compared with successive two-photon ionization. Similarly, Yamanaka et al.[24] also attributed their charge generation to CT exciton dissociation but with the help of SOP (Figure 3h). SOP describes an assisted photoinduced charge-separation process: when the EML is fabricated, host or guest molecules may form region with molecular alignment (or crystallization) and generate regional potential because of the permanent dipole moments of these molecules. The local potential can help the CT excitons of the TADF emitters to dissociate and generate charges.

In order to probe the OLPL mechanism for our system, we measured excitation-intensity-dependent OLPL decay curves of the 0.5 wt% CzPhAP:PPT film. The film was excited using a 365 nm LED for 1 min with different excitation intensities ranging from 0.7 to 23.2 mW cm^{-2}. The results presented in Figure 3h show that using the 23.2 mW cm^{-2} excitation intensity gave OLPL duration around 4000 s. For low excitation intensity (0.7 mW cm^{-2}), only around 10 s emission duration was observed. We attribute this to the photogeneration of far fewer separated charges at low excitation intensity which may suggest that the charge separation in this system is a multi-photon process. In addition, CzPhAP has a large ΔE_{ST} and high molecular rigidity which contribute to a long-lived T_1. Therefore, successive two-photon ionization is most likely to be the mechanism responsible for our OLPL. In CzPhAP-doped films, Optical excitation leads to the generation of long-lived triplets, which can then be further excited, leading to ionization. A long-lived triplet excited state is important because it enables a substantial population of triplets to build up, which increases the chance of a second photon being absorbed. To verify this explanation, we tested some other emitters that have much shorter T_1 lifetime, namely 4CzIPN,[35] DCzIPN,[36] and Alq_3. Each of these materials was doped into PMMA, but OLPL was not observed. This is consistent with the successive two-photon ionization mechanism for OLPL.

In summary, we have demonstrated that an inefficient TADF compound, CzPhAP, doped in PPT, TPBi, and PMMA matrices can also show room-temperature OLPL lasting for thousands of seconds. Importantly the OLPL does not need bi-molecular exciplex formation. CzPhAP is ideal for OLPL applications because it has a large ΔE_{ST} and it is a very rigid molecule, both of which contribute to its long T_1 lifetime and the consequently large T_1 populations. This large T_1 population is ideal for photoinduced charge generation through successive two-photon ionization processes. Moreover, we studied the origin of the two regimes in the decay curves of 0.5 wt% CzPhAP in PPT, TPBi, and PMMA. We found that in the short-time regime (1–5 s for the PPT and TPBi films, 1–7 s for the PMMA film) the emission is from both the S_1 and T_1 states of CzPhAP. In the long-time regime (>5 s), the emission is from the S_1 state of the emitter for the PPT and TPBi films. This means that care needs to be taken when using the onset of the 77 K afterglow spectrum from a TADF-emitter-doped film to determine the emitter's T_1 energy level, because there could also be a contribution to the emission from singlets formed through charge recombination.

In this work, we also found that many OLPL properties depend on the host material. For example, at 300 K, we found the OLPL decay slopes in log–log plot vary from –0.55 to –1

in different hosts, and attributes this to different durations of charge trapping on the different hosts. At 77 K, the charge-recombination rate in the PMMA film is so low that S_1 emission can hardly be seen in the 1–10 ms time window, which is completely different from the PPT and TPBi cases. As host materials consist of 99.5 wt% of our films, and are responsible for trapping photo-induced charges, they certainly have a strong influence on the OLPL performance. Some of these effects have been studied by Ohkita et al. through using different polymers as hosts in 1997,[31] leading to different decay slopes and durations of OLPL. However, the main focus of our work is to demonstrate that putting a TADF emitter into readily available hosts (including PMMA) is another way to realize long-lived room-temperature OLPL. Therefore, more detailed host material dependency was not further studied.

Last but not least, we demonstrated that the cheap polymer PMMA could also be employed as a room-temperature OLPL host, which opens the door to cost-effective OLPL materials. Although Ohkita et al.[15] have already demonstrated that doping perylene in PnBMA can also realize OLPL at room temperature, our work shows CzPhAP can show emission duration in PMMA that is twice as long. Moreover, combining the flexible design of TADF emitters, further expanding this strategy may lead to better OLPL systems with more emission colors and longer afterglow durations. Furthermore, although the OLPL was observed to be quenched in air, it can survive in inert gas environment. This indicates that encapsulation will enable OLPL in the ambient environment. Therefore, by combining the low cost of PMMA manufacture with flexible designs of TADF molecules, pure organic, large-scale, color tunable, and low-cost room-temperature OLPL applications are possible.

Experimental Section

Fabrication of the CzPhAP:PPT/TPBi Films (0.5 wt%): CzPhAP powders were mixed with PPT/TPBi powders according to the doping concentration inside glass vials. The glass vials were transferred into the glove box for the nitrogen environment. The powder on the glass substrates were transferred to a hotplate which was heated up to 250 °C. When the powder completely melted, the glass substrates were removed from the hotplate for a quick cool down.

Fabrication of the CzPhAP:PMMA Film (0.5 wt%): CzPhAP powders were dissolved in PMMA's monomer, MMA, according to the doping concentration in a glass vial with the dissolving temperature around 50 °C with the help of magnetic stirring bar. AIBN (0.1 wt%) was mixed as the radical initiator, and the glass vial was heated up to 60 °C in oil bath for 5 h under N_2. The temperature was increased to 110 °C for 1 h, and then to 160 °C for 1 h to completely polymerize MMA. The glass vial was put under vacuum ($<10^{-2}$ mbar), and the temperature was increased to 200 °C for 3 h to remove all the remaining potential liquid. The final product was left in N_2 during the cooling down process.

Short-time range (<2 s) PL decay was measured using a fluorimeter (Edinburgh Instruments F980). Long-time range (>2 s) PL decay was measured using a SiPM (C13366-1350GA, Hamamatsu photonics).

Short-time range (<10 ms) TRPL spectra were measured using an intensified CCD (ICCD, Stanford Computer Optics, 4Picos). Long-time range (>1 s) TRPL spectra were measured using Andor CCD (DV420-BV).

Long-Persistent Luminescence Measurement Conditions: The LPL decay curves were measured in the same setup described in ref. [17]. The sample was placed in a cryostat (PS-HT-200, Nagase Techno-Engineering) connected to active turbo pump (HiPace80, Pfeiffer Vacuum). The excitation source was a 365 nm LED (M365L2, Thorlabs) with an LED driver (LEDD1B, Thorlabs). The samples were excited for 60 s or longer with a certain driving current before the emission detection, and afterglow of the sample was detected by a SiPM (C13366-1350GA, Hamamatsu photonic).

Supporting Information

Supporting Information is available from the Wiley Online Library or from the author.

Acknowledgements

The authors are grateful to the EPSRC for financial support (grants EP/P010482/1, EP/R035164/1, and EP/L017008/1). The authors gratefully acknowledge a Leverhulme Trust Research Grant (RPG-2017-231). The authors thank Umicore for the gift of materials. The authors thank the EPSRC UK National Mass Spectrometry Facility at Swansea University for analytical services. The authors thank the Japan Science and Technology Agency (JST), ERATO, Adachi Molecular Exciton Engineering Project, under JST ERATO Grant Number JPMJER1305; JSPS Core-to-Core Program; JSPS KAKENHI Grant Numbers JP18H02049 and JP18H04522; and the International Institute for Carbon Neutral Energy Research (WPI-I2CNER) sponsored by the Ministry of Education, Culture, Sports, Science and Technology (MEXT). The authors thank Dr. Pavlos Manousiadis for taking the photos. The authors thank Drs. Dianming Sun, Kou Yoshida, Arvydas Ruseckas, Paloma dos Santos, and Zesen Lin for useful discussions. The authors thank Mr. Cheng Lian and Ms. Mengjie Wei for their help with the PL spectra measurement. W.L., Z.L., and C.S. thank the China Scholarship Council (grant numbers 201708060003, 201703780004, and 201806890001). A.K. Gupta thanks Newton Fellowship NF171163. The research data supporting this publication can be accessed at https://doi.org/10.17630/1fdb4634-0c6b-4ca4-bfa8-436b8b2c42bf.

Conflict of interest

The authors declare no conflict of interest.

Keywords

afterglow, charge recombination, charge separation, long-persistent luminescence (LPL), organic long-persistent luminescence (OLPL), thermally activated delayed fluorescence (TADF)

Received: June 8, 2020
Revised: July 30, 2020
Published online:

[1] J. Hölsä, *Electrochem. Soc. Interface* **2009**, *18*, 42.
[2] T. Matsuzawa, Y. Aoki, N. Takeuchi, Y. Murayama, *J. Electrochem. Soc.* **1996**, *143*, 2670.
[3] H. Yamamoto, T. Matsuzawa, *J. Lumin.* **1997**, *72–74*, 287.
[4] S. Xu, R. Chen, C. Zheng, W. Huang, *Adv. Mater.* **2016**, *28*, 9920.
[5] S. Hirata, M. Vacha, *Adv. Opt. Mater.* **2017**, *5*, 1600996.
[6] R. Kabe, N. Notsuka, K. Yoshida, C. Adachi, *Adv. Mater.* **2016**, *28*, 655.
[7] S. Hirata, K. Totani, J. Zhang, T. Yamashita, H. Kaji, S. R. Marder, T. Watanabe, C. Adachi, *Adv. Funct. Mater.* **2013**, *23*, 3386.
[8] C.-R. Wang, Y.-Y. Gong, W.-Z. Yuan, Y.-M. Zhang, *Chin. Chem. Lett.* **2016**, *27*, 1184.

[9] J. Yang, X. Zhen, B. Wang, X. Gao, Z. Ren, J. Wang, Y. Xie, J. Li, Q. Peng, K. Pu, Z. Li, *Nat. Commun.* **2018**, *9*, 840.
[10] W. Jia, Q. Wang, H. Shi, Z. An, W. Huang, *Chem. - Eur. J.* **2020**, *26*, 4437.
[11] J. L. Kropp, W. R. Dawson, *J. Phys. Chem.* **1967**, *71*, 4499.
[12] K. Jinnai, N. Nishimura, R. Kabe, C. Adachi, *Chem. Lett.* **2019**, *48*, 270.
[13] Z. Lin, R. Kabe, N. Nishimura, K. Jinnai, C. Adachi, *Adv. Mater.* **2018**, *30*, 1803713.
[14] R. Kabe, C. Adachi, *Nature* **2017**, *550*, 384.
[15] H. Ohkita, W. Sakai, A. Tsuchida, M. Yamamoto, *Bull. Chem. Soc. Jpn.* **1997**, *70*, 2665.
[16] H. Ohkita, W. Sakai, A. Tsuchida, M. Yamamoto, *Macromolecules* **1997**, *30*, 5376.
[17] K. Jinnai, R. Kabe, C. Adachi, *Adv. Mater.* **2018**, *30*, 1800365.
[18] Z. Lin, R. Kabe, K. Wang, C. Adachi, *Nat. Commun.* **2020**, *11*, 191.
[19] Y. Yuan, Y. Hu, Y.-X. Zhang, J.-D. Lin, Y.-K. Wang, Z.-Q. Jiang, L.-S. Liao, S.-T. Lee, *Adv. Funct. Mater.* **2017**, *27*, 1700986.
[20] Y. Hu, Y. Yuan, Y.-L. Shi, D. Li, Z.-Q. Jiang, L.-S. Liao, *Adv. Funct. Mater.* **2018**, *28*, 1802597.
[21] J. Xue, Q. Liang, R. Wang, J. Hou, W. Li, Q. Peng, Z. Shuai, J. Qiao, *Adv. Mater.* **2019**, *31*, 1808242.
[22] D. G. Congrave, B. H. Drummond, P. J. Conaghan, H. Francis, S. T. E. Jones, C. P. Grey, N. C. Greenham, D. Credgington, H. Bronstein, *J. Am. Chem. Soc.* **2019**, *141*, 18390.
[23] S. M. Shinde, G. Kalita, M. Tanemura, *J. Appl. Phys.* **2014**, *116*, 214306.
[24] T. Yamanaka, H. Nakanotani, C. Adachi, *Nat. Commun.* **2019**, *10*, 5748.
[25] P. Debye, J. O. Edwards, *J. Chem. Phys.* **1952**, *20*, 236.
[26] G. C. Abell, A. Mozumder, *J. Chem. Phys.* **1972**, *56*, 4079.
[27] W. H. Hamill, K. Funabashi, *Phys. Rev. B* **1977**, *16*, 5523.
[28] H. Scher, E. W. Montroll, *Phys. Rev. B* **1975**, *12*, 2455.
[29] M. Tachiya, A. Mozumder, *Chem. Phys. Lett.* **1975**, *34*, 77.
[30] G. Méhes, K. Goushi, W. J. Potscavage, C. Adachi, *Org. Electron.* **2014**, *15*, 2027.
[31] H. Ohkita, W. Sakai, A. Tsuchida, M. Yamamoto, *J. Phys. Chem. B* **1997**, *101*, 10241.
[32] M. Yamamoto, H. Ohkita, S. Ito, *Chin. J. Polym. Sci.* **2001**, *19*, 129.
[33] M. Yamamoto, H. Ohkita, W. Sakai, A. Tsuchida, *Synth. Met.* **1996**, *81*, 301.
[34] H. Ohkita, T. Koizumi, W. Sakai, T. Osako, M. Ohoka, M. Yamamoto, *Chem. Phys. Lett.* **1997**, *276*, 297.
[35] H. Uoyama, K. Goushi, K. Shizu, H. Nomura, C. Adachi, *Nature* **2012**, *492*, 234.
[36] Y. J. Cho, K. S. Yook, J. Y. Lee, *Sci. Rep.* **2015**, *5*, 7859.